



Numerical modeling of the behavior of multiple-cable-pylon cap joint in a cable roof structure

W.A. Salah Khalil¹, M.A. Gizejowski², S. Wierzbicki³

¹ PhD, Al Azhar University, Engineering Faculty, Civil Engineering Department, Cairo, Egypt

² PhD, DSc, Warsaw University of Technology, Warsaw, Poland

³ PhD, DSc, Warsaw University of Technology, Warsaw, Poland

المخلص:

يقدم هذا البحث محاكاة عددية تفصيلية باستخدام طريقة العناصر المحددة لوصلة كاب برج معدني متعدد الكابلات في سطح معلق بالكابلات في مشروع حقيقي. تم نمذجة المنشأ ككل كنظام ثلاثي الأبعاد يتكون من عناصر الكابلات المرنة لنقل قوى الشد، وعناصر كمرية لتمثيل مكونات النظم الإنشائية للبرج. تم إختيار الجزء العلوي فقط من البرج لعمل دراسة تحليلية موضعية لسلوك وصلة كاب البرج مع الكابلات. تم تمثيل جميع المكونات الأنبوبية المعدنية باستخدام العناصر القشرية الرقيقة. تم عمل تحليل مرن عددي للاستقرار المتشعب لوصلة كاب البرج المعدني وذلك بغرض تمثيل التشوهات الكائنة في الشكل محل الدراسة. تم إختيار الشكل الإنبعاجي الأول ليمثل التشوهات الموجودة في الأبعاد في حالة عدم تطبيق أية أحمال. تم تطبيق خاصية التحميل عن طريق الإزاحة باستخدام طريقة Riks للتحليل مع الأخذ في الإعتبار الخصائص غير الخطية لكل من خامات وأبعاد نموذج المحاكاة المقترح. وأخيرا تم تقديم توصيات مهمة من وجهة النظر العملية والتطبيقية.

ABSTRACT

This research introduces a detailed finite element modeling for a multiple-cable-to-pylon cap joint of a real cable roof structure. The considered steel cap joint structure is numerically modeled as a 3D system composed of flexible cable elements, transferring tensile forces, and beam elements delineating ring and compound pylon structural systems. The upper part substructure of the pylon, pylon cap joint, is chosen to investigate the localized behavior of the pylon cap joint being exposed to a set of internal forces obtained from such a simple finite element (FE) modeling. All the steel tubular components of the analyzed pylon substructure are simulated using thin shell elements. The elastic bifurcation stability is conducted as a first step analysis to picture the imperfect geometry of the analyzed substructure. The first buckling mode shape is considered for the imperfect geometry at the unloaded condition. The geometrically and materially nonlinear Riks analysis available in ABAQUS software is employed to evaluate the load-displacement characteristics of the developed imperfect structure model. Remarkable conclusions are introduced considering the practical applications point of view.

1 INTRODUCTION

1.1 General

Steel cable and membrane structures can represent the ideal solution for the large spans without internal supports. This type of structural system is adopted in such a way that the system demonstrates a capability to transmit all internal actions by pre-tensioned cable elements, as well as by the compression ring and pylon supporting

structure. Such kind of systems have been presented to be as successful as the textile surface membrane structures and reinforced concrete shell-like structures.

Taking into account structural safety and integrity, surface membrane elements and linear cable elements have to conform to specific weight and balance requirements, and above all – the requirements of strength, stiffness and durability that enable the stress distribution to be corresponded to external loading conditions in an elastic behavior, without immoderate localized plastic deformations in the steel supporting structures. Problems of force transmitting in cable roof structures have to be dealt with a great care and an accurate attention needs to be paid to the localized stress concentrations and stiffness behavior of cable supporting elements.

1.2 *Structure considered*

This research introduces a comprehensive FE modeling of the multiple-cable-to-pylon cap joint of a real project. The layout of the roof, supporting structure of which is the primary concerned hereafter, is presented in Figure 1.



Figure 1. Roof and pylons of amphitheatre structure considered.

The supporting structure for cables consists of the ring system supported by columns of one side of the roof and two pylons supporting the cables restraining the ring on the other side. Each compound pylon consists of three chord tubular elements that meet together at the top and bottom of the pylon, ensuring that pylon as a whole behaves as leaning compound column. The cap pylon joint holding the ring cables is rather of a complex detailing as it is presented in Figure 2. The cap joint of the pylon that was prepared for erection is shown in Figure 2. After assembling of the entire structure, the roof was subjected to actions before the final inspection for service designation. Inspection of the structure detected cracks in the walls of the tubular member, close to the vicinity of cap member welded connections.

1.3 *Design and construction aspects*

The structure as a whole was modeled as a 3D system composed of flexible cable elements, transmitting tensile forces, and beam elements representing ring and compound pylon structural elements. Pylon joints were not considered in details in the

design project and dimensioned without a dequate advanced analysis for the effects of localized yielding of joint components under service loads. The number of intersecting elements located in a small area of the cap joint, caused the difficulties to ensure required fitting tolerances and a good quality of welded connections during manufacturing.

Investigations were conducted into the behavior of the cap joint in its primary designed version shown in Figure 2, and in addition to other two strengthened versions that were suggested by the design office (joints reinforced by additional conical elements holding the cable guiding tubes).

The set of the internal forces acquired from modeling of the upper part of the pylon is selected for the detailed analysis of localized behavior of the pylon cap joint. The joint accommodates guiding CHS elements for the roof cables anchored in the pylon and the pylon upper CHS spire element provided for a safe load transfer from the roof cables onto the compound pylon composed of three chords and battens of tubular sections. Figure 3 depicts the pylon and its subsystem with the cap joint analyzed in this research for failure modes, strength and plastic zones in the ultimate state.



Figure 2. Details of pylon cap joint before erection.

2 NUMERICAL MODELING

2.1 Scope of investigations and modeling technique

FE modeling technique is presented hereafter that allows for prediction of the behavior of pylon cap joint. All the steel tubular components of the analyzed pylon substructure are simulated using of thin shell four nodes and three nodes elements. Three different joint solutions are analyzed:

1. The original solution with the short conical shell.

2. The strengthened solution 1 with the original short conical shell reinforced from outside by a longer conical shell of 16 mm thickness welded to the spire tube, cable guiding tubes and the joint bottom plate.
3. The strengthened solution 2 with an additional reinforcing cover shell of 20 mm in thickness welded to the longer conical shell.

Summary of numerical model features applied for analyzed joint solutions are given in Table 1. Three different methods of analysis are employed. Numerical simulations are supported by commercial software ABAQUS. In order to find the sensitivity of analyzed subsystems to buckling effects and describe a possible profile of initial imperfections, the linear buckling analysis (LBA) is conducted. The first buckling mode is chosen for the description of the pylon imperfect geometry in the unloaded condition. Load-displacement characteristics are evaluated using the Riks type analysis in two versions: geometrically and materially nonlinear analysis – GMNA (perfect model) and GMNIA – geometrically and materially nonlinear analysis with imperfections (imperfect model).

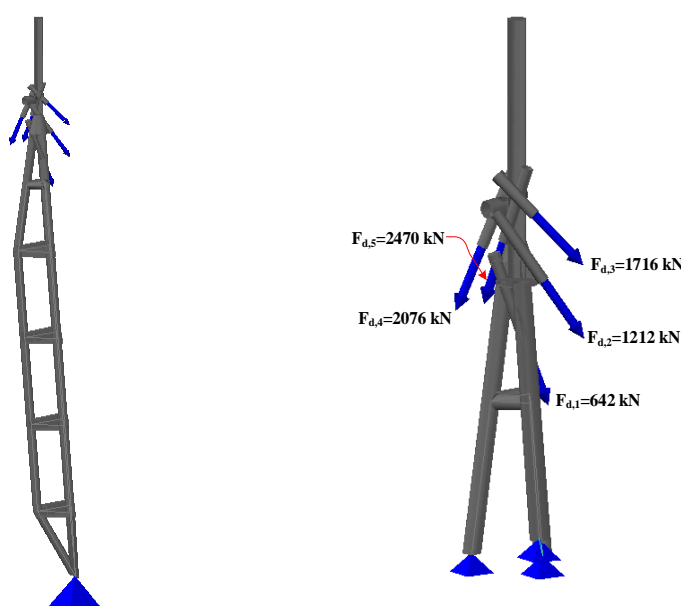


Figure 3. Structural system analyzed

Table 1. Summary of numerical model

| solution | No. of nodes overall | No. of shell elements | |
|----------------|----------------------|-----------------------|----------------|
| | | 4 node element | 3 node element |
| 1 [*] | 36732 | 37007 | 84 |
| 2 [*] | 39967 | 40075 | 91 |
| 3 [*] | 41089 | 41348 | 92 |

* As identified above the table

2.2 Numerical results from LBA

Load factors are referenced to the design (factored) load level of the critical combination of actions. Figure 4 displays the buckling mode corresponding to the critical load factor 4.99. This mode is of the global-local nature and indicates that the local buckling of a weak short conical shell is associated with buckling of the upper

spire part of the pylon. Higher buckling modes are similar to the first one. The second and third modes are characterized by bifurcation load factors 5.32 and 5.85.

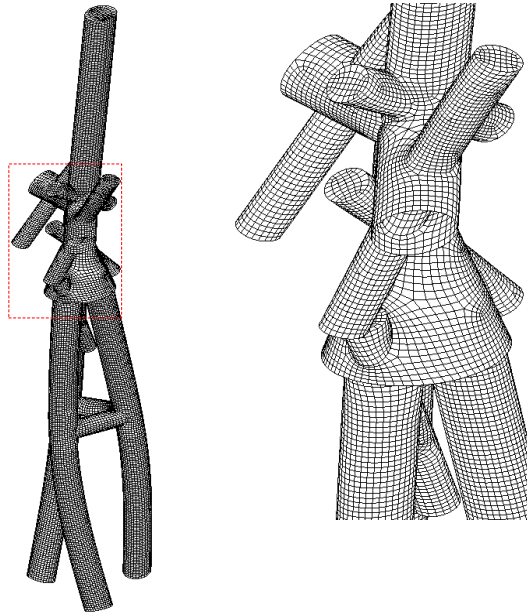


Figure 4. First buckling mode – joint solution 1

Similar analysis is carried out for the strengthened joint solution 2. The first buckling mode shows a smaller contribution of the spire deformation to the buckling state, and more pronounced are local ones. Figure 5 shows this buckling load factor 5.23. The strengthened joint solution 2 is characterized by a higher buckling load factor if compared with that of solution 1 but the first buckling mode remains similar to that of solution 1. The higher buckling modes are of similar forms but they are associated with the local buckling rather than global. Bifurcation load factors corresponding to higher buckling modes are 6.00 and 6.62. The similar behavior to that of solution 2 shows also the joint solution 3.

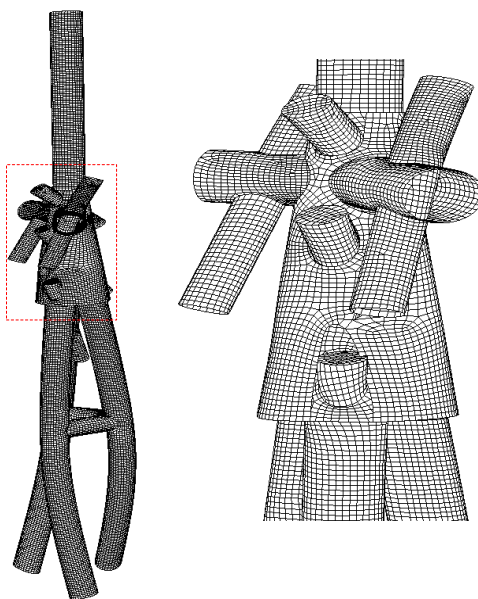


Figure 5. First buckling mode – joint solution 2

2.3 Numerical results from GMNA and GMNIA

Results are presented in terms of the load displacement characteristic. The load factor of the critical combination of actions is plotted against the resultant spire displacement. Results for the joint solution 1 are presented in Figure 6 where the following notation is used: *Unstiff* – perfect model, *Unstiff-GI* – geometrically imperfect model.

From the results presented in Figure 6 it can be concluded that the cap joint in the original solution is inadequate. The failure load factor from both GMNA and GMNIA analyses are below unity. It is worth to note that the effect of geometric imperfections is not important from the safety point of view. Figure 7 presents the map of Huber-Mises stresses indicating almost the complete yielding of the spire tubular member and cable guiding tubes within the cap joint area.

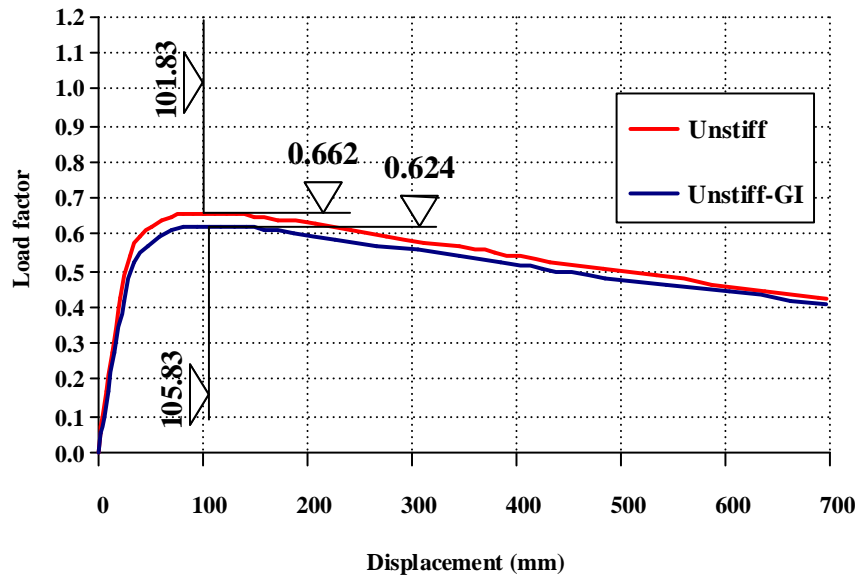


Figure 6. Equilibrium paths for joint solution 1

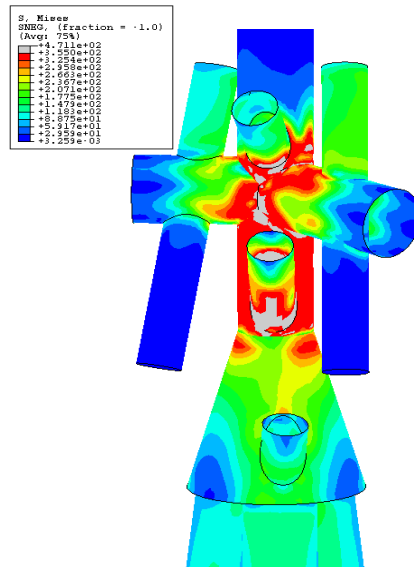


Figure 7. Map of Huber-Mises stresses from Unstiff-GI model at the ultimate state of joint solution 1

Similar analysis is performed for solution 2 and 3. Results for the joint solution 2 are presented in Figure 8 where the following notation is used: *Stiff* – perfect model, *Stiff-GI* – geometrically imperfect model.

From the results presented in Figure 8, one can conclude that the cap joint in the joint solution 2, reinforced with longer conical shell, is adequate in terms of overall performance under static (one cycle) loading. The failure load factor from both GMNA and GMNIA analyses are above unity. Moreover, like in the cap joint solution 1, the effect of geometric imperfections is not important from the joint safety point of view. Figure 9 presents the map of Huber-Mises stresses indicating excessive yielding zones in joint components at the ultimate state. The yielding zones in joint components common for solutions 1 and 2 are practically of the same spread.

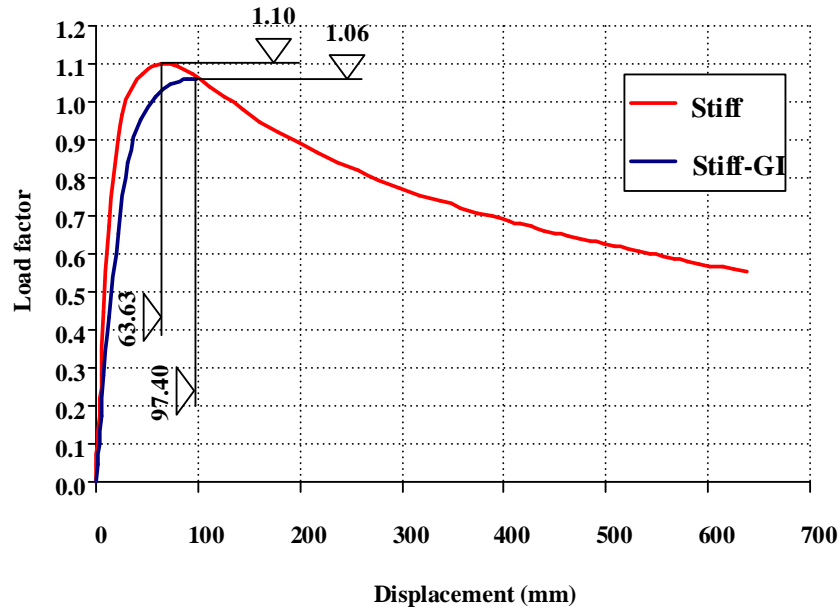


Figure 8. Equilibrium paths for joint solution 2

Results for the joint solution 3 are presented in Figure 10 where the notation *D-Stiff-GI* means doubly reinforced and geometrically imperfect model. Figure 11 shows the map of Huber-Mises stresses indicating that the yielding zones are less advanced at the load factor of 1.1 than those of solution 2 at the ultimate state.

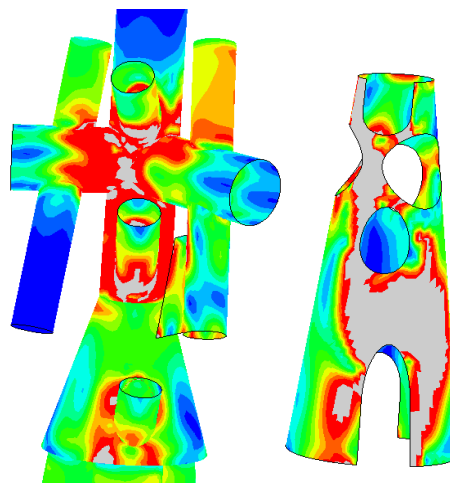


Figure 9. Map of Huber-Mises stresses from *Stiff-GI* model at the ultimate state of joint solution 2

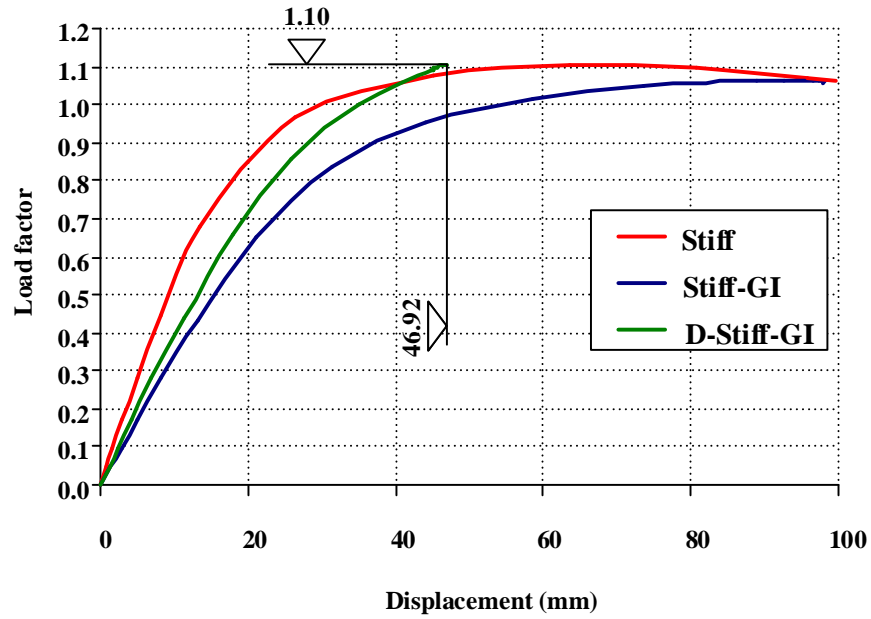


Figure 10. Equilibrium paths for joint solution 2

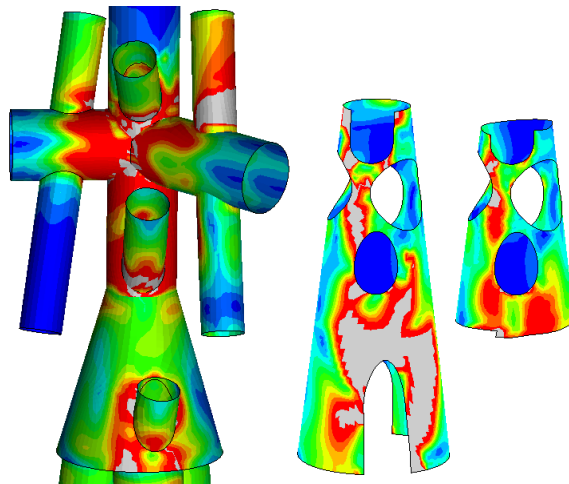


Figure 11. Map of Huber-Mises stresses from D-Stiff-GI model at the load factor 1.1 for joint solution 3.

3 CONCLUSIONS

Aspects of advanced analysis of complex cap joint of the pylon supporting the cable roof are presented in this paper. Original joint solution was developed without the detailed finite element analysis that would reproduce a complex behavior of the joint both at the ultimate and serviceability limit states. It is proven that the joint is overstressed. The failure load factor is below unity (failure occurs under the design load level).

The insufficient strength of the pylon cap joint was the reason for important proposals of the joint detailing in order to fulfill the limit state criteria at both the ultimate and serviceability limit states. Reinforcements were provided to the original solution in terms of conical shells, longer in the solution 2 and in the solution 3 – additional shorter and welded to it. Reinforced joints are characterized by the ultimate load factor above unity, therefore providing acceptable reliability at the ultimate limit state.

It has to be emphasized that to avoid failure under alternating loading, the cap joint has to be under a very limited plastic deformations, if not entirely elastic in the serviceability limit state. This requirement is not discussed in details in this paper.

4 REFERENCES

- [1] .Seidel, M. 2009, "*Tensite Surface Sstructures*", *A Practical Guide to Cable and Membrane Construction*. Berlin. Ernst & Sohn
- [2] Katherina Santoso, "Wide-Span Cable Structures", Master thesis, 2003
- [3] Vaneeta Devi1, A.K.Ahuja, "Constructional Design Consideration for Long Span Flexible Circular Grid Roofs", *IOSR Journal of Mechanical and Civil Engineering (IOSR-JMCE)*, Volume 11, Issue 2 Ver. VII (Mar-Apr. 2014), pp. 01-05, 2014.
- [4] Hibbitt, Karlson, Sorenson, "ABAQUS User's Manual" Version 6.14, Part 1&2, 2014.